2017

A review of phosphorus partition relations for use in basic oxygen steelmaking

Phillip Drain
University of Wollongong, pbd150@uowmail.edu.au

Brian J. Monaghan
University of Wollongong, monaghan@uow.edu.au

Guangqing Zhang
University of Wollongong, gzhang@uow.edu.au

Raymond Longbottom
University of Wollongong, rayl@uow.edu.au

Michael W. Chapman
BlueScope Steel Limited, michael.w.chapman@bluescopesteel.com

See next page for additional authors

Publication Details

Drain, P. B., Monaghan, B. J., Zhang, G., Longbottom, R. J., Chapman, M. W. & Chew, S. J. (2017). A review of phosphorus partition relations for use in basic oxygen steelmaking. Ironmaking and Steelmaking, 44 (10), 721-731.

A review of phosphorus partition relations for use in basic oxygen steelmaking

Abstract
Phosphorus removal in basic oxygen steelmaking is a significant problem for integrated steelmakers. Phosphorus removal is required due to its deleterious effect on the mechanical properties of steel. However, this is progressively becoming more difficult due to the increasing phosphorus content of many iron ores. Many studies have investigated dephosphorisation and published empirical phosphorus partition (L_P) equations for a range of conditions. The structure of these equations has been used to develop a new partition relation that allows the effect of minor slag constituents such as TiO_2, Al_2O_3 and V_2O_5 on steel dephosphorisation to be tested. Al_2O_3 was found to have a weak negative effect on the measured L_P, except at the lower oxygen potential range tested, where a positive correlation was observed. Increasing TiO_2 and V_2O_5 contents were found to decrease the measured L_P; however, these correlations became less prevalent at the higher oxygen potential ranges tested.

Disciplines
Engineering | Science and Technology Studies

Publication Details
Drain, P. B., Monaghan, B. J., Zhang, G., Longbottom, R. J., Chapman, M. W. & Chew, S. J. (2017). A review of phosphorus partition relations for use in basic oxygen steelmaking. Ironmaking and Steelmaking, 44 (10), 721-731.

Authors
Phillip Drain, Brian J. Monaghan, Guangqing Zhang, Raymond Longbottom, Michael W. Chapman, and Sheng Chew

A Review of Phosphorus Partition Relations for Use in Basic Oxygen Steelmaking

Phillip B. Drain[1,2]*, Brian J. Monaghan[1,2,4], Guangqing Zhang[1,2,5], Raymond. J. Longbottom[1,2,6], Michael W. Chapman[1,3,7], Sheng J. Chew[1,3,8]

[1] ARC Research Hub for Australian Steel Manufacturing, University of Wollongong, Wollongong, NSW, 2522, Australia.

[2] University of Wollongong, School of Mechanical, Materials, Mechatronics and Biomedical Engineering , Wollongong, NSW, Australia, 2522

[3] BlueScope Steel, Iron & Steelmaking Technology, Port Kembla NSW.

*Corresponding author. Email: pbd150@uowmail.edu.au

[4] Email: monaghan@uow.edu.au

[5] Email: gzhang@uow.edu.au

[6] Email: rayl@uow.edu.au

[7] Email: Michael.Chapman2@bluescopesteel.com

[8] Email: Sheng.Chew@bluescopesteel.com

Abstract

Phosphorus removal in basic oxygen steelmaking (BOS) is a significant problem for integrated steelmakers. Phosphorus removal is required due to its deleterious effect on the mechanical properties of steel. However, this is progressively becoming more difficult due to the increasing phosphorus content of many iron ores.

Many studies have investigated dephosphorisation and published empirical phosphorus partition (L_P) equations for a range of conditions. The structure of these equations have been used to develop a new partition relation that allows the effect of minor slag constituents such as TiO_2, Al_2O_3 and V_2O_5 on steel dephosphorisation to be tested.

Al_2O_3 was found to have a weak negative effect on the measured L_P, except at the lower oxygen potential range tested, where a positive correlation was observed. Increasing TiO_2 and V_2O_5 contents were found to decrease the measured L_P, however these correlations became less prevalent at the higher oxygen potential ranges tested.

Keywords: basic oxygen steelmaking (BOS), dephosphorisation, phosphorus partition, slags.

Definitions and Nomenclature

( ) = in slag solution

[ ] = in liquid iron solution

%i = mass % of i

(%Fe_t) = mass% of total Fe in slag phase

(%Fe_tO) = mass% of total Fe in slag phase as FeO

M_i = molecular weight of oxide i

R = universal gas constant, 8.314 $JK^{-1}mol^{-1}$

N = mole fraction of oxide or ion

y_i = L_P calculated by model

$\hat{y}_i$ = L_P calculated by linear regression line through results to the origin

Λ = optical basicity of slag

Λ_i = optical basicity of single oxide of species i

T = Temperature in K

1. Introduction

The deleterious effect of phosphorus on steel properties and the increasing content of phosphorus in iron ores are key drivers in the ongoing research in steel dephosphorisation [1, 2]. Phosphorus removal in the steelmaking process can be represented by the ionic or molecular reactions given in equations (1) and (2), respectively. These equations show phosphorus activity in the metal, oxygen potential and slag basicity play a critical role in phosphorus removal from steel.

$$[P]+\frac{5}{2}[O]+\frac{3}{2}\left(O^{2-}\right)=\left(PO_4^{3-}\right) \qquad (1)$$

$$2[P] + 5[O] = (P_2O_5) \qquad (2)\ [3]$$

Temperature also has a significant effect on phosphorus removal as shown by the Gibbs free energy of reaction (2) as given in equation (3).

$$\Delta G° = -832384 + 632.65T\ Jmol^{-1} \qquad (3)\ [3]$$

Considering equations (1) and (2), phosphorus removal from iron and steel is promoted by high [P] activity, high oxygen potential [O] and high basicity (O^{2-}). From equation (3) it can be seen that lowering temperature increases the thermodynamic driving force for phosphorus removal by decreasing ΔG°.

Unfortunately, for integrated steelmakers, there is no step in the process where all of these conditions are met. Dephosphorisation is typically carried out in either hot metal pre-treatment (low temperature, high O^{2-} but low pO_2) or in the basic oxygen steelmaking (BOS) converter (high temperature, high O^{2-} and high pO_2) [4-7]. The temperature of the BOS process is dictated by other factors than phosphorus control or partition [4-7]. If ultra-low phosphorus steel is required, it is also possible to remove phosphorus from the steel through secondary refining processes [8, 9].

For dephosphorisation it is known that the controlling oxygen potential represents a dynamic relation between the iron oxide in the slag and the carbon in the hot metal/steel [4, 5, 10-17]. Operational BOS models predicting phosphorus removal often approximate this to a factor that represents the slag iron oxide content such as Fe_tO, or Fe_t.

There are many approaches for evaluating slag basicity that range from empirical plant relations to those founded on thermodynamic and slag structure fundamentals. A full review of these is beyond the scope of this study. The use of the simple V-ratio relation (equation 4) or similar composition acid-base approaches (e.g. equation (5)) is well established by steelmakers. Optical basicity (Λ), as given in equation (6), offers a relatively simple and convenient approach to calculating a single number that represents slag basicity. Optical basicity takes into account the effect of minor slag constituents (such as TiO_2 or V_2O_5) on the basicity.

$$V = \frac{\%CaO}{\%SiO_2} \quad (4) \quad [18]$$

$$B = \frac{N_{CaO} + N_{MgO}}{N_{SiO_2} + 1.05 N_{AlO_{1.5}}} \quad (5) \quad [19]$$

$$\Lambda = N_i \Lambda_i + N_j \Lambda_j + \cdots \quad (6) \quad [18]$$

Dephosphorisation has been studied extensively, with over 90 different empirical correlations of dephosphorisation equilibria or effective equilibria[2, 3, 19-94]. These empirical relations are often useful for optimising dephosphorisation in the BOS. However, they are often limited to specific temperature and compositional ranges, or kinetic conditions for which they were developed. Relations developed using industrial data are further limited by being only estimates of the effective equilibria reached under the specific kinetic regime and furnace type for which they were developed. The kinetics of phosphorus removal in BOS process can be affected by, amongst other factors, bath stirring, lance height and design, blow time, and physical properties of slag.

The aim of this study is to develop a phosphorus removal relation that can be used to isolate the effect of minor slag constituents (e.g. TiO_2, Al_2O_3 and V_2O_5). Although published empirical phosphorus partition models are often limited to the conditions for which they were developed, their structure and component coefficients can be used to inform the basicity and oxygen potential representations for a new model. Thus, a two stage approach to model development has been used. In the first stage, published phosphorus partition relations will be assessed using a large industrial dataset to determine which equation best represents the data. In the second stage the focus is to develop a new equation,

determining which representations of temperature, oxygen potential and slag basicity are most appropriate by regression against the large industrial dataset. While this new L_P relation will suffer similar limitations to other plant data derived relations, it will be optimised for the industrial dataset used in this study, thus it may enable testing of the thermodynamic and kinetic effects of minor slag constituents on dephosphorisation.

2. Selection and Filtering of Industrial Data

A filtered dataset of steel and slag compositions, and processing conditions was collated for 11340 heats (dataset 1) from the BlueScope Port Kembla BOS plant. Arc optical emission spectroscopy, sub-lance EMF [O] and X-ray fluorescence were used to obtain compositional data for steel and slag samples, respectively. Samples were obtained routinely via a sub-lance (metal) and from a chill/dip sample (slag). The dataset does not include any heats with incomplete records or unusual processing conditions, including:

- Incomplete data for heat duration, temperature, slag or metal compositions.
- Unknown slag mass due to either de-siliconisation or high quantities of slag remaining in the converter from the previous blow.
- Heats with high pO_2 due to re-processing of steel from secondary refining.

A model cannot be accurately assessed against the dataset it was fitted to, as it is likely to outperform models not fitted to the data. Thus, a calibration/fitting dataset and an independent test were required. Consequently, dataset 1 was split arbitrarily into dataset 2 (11274 heats for tuning/fitting the models) and 3 (66 heats for assessing the performance of the model). The larger dataset was used for fitting the models to maximise their fit across a wide range of operating conditions.

3. Methodology and Results

3.1 Evaluation of Published Phosphorus Partition (L_P) Equations

The limits of phosphorus removal are given by the dephosphorisation equilibria or effective equilibria. These may be represented in several ways, such as equilibrium constants, phosphate capacities or different forms of the phosphorus partition (L_P). In this study the effective equilibria is defined by the L_P, as defined in equation (7). Where equations from

other studies are presented, any (effective) dephosphorisation equilibrium term has been converted to L_p as given in equation (7).

$$L_P = \frac{(\%P)}{[\%P]} \qquad (7)$$ [95]

Thirty six published L_P equations (Table 1) were selected for testing from over 90 published L_P equations collated for this study[2, 3, 19-94, 96]. Equations chosen for further evaluation were selected if they satisfied one or more of the following criteria:

- Recently published (2000 onwards) using either laboratory or industrial data.
- The L_P equation was derived using industrial data.
- The L_P equation included minor BOS slag constituents (e.g. TiO_2, Al_2O_3, and V_2O_5).
- The L_P equation included optical basicity as an input, allowing the effect of minor slag constituents to be easily incorporated.

Equations were disregarded using the following criteria:

- The L_P equation included slag additions no longer used for environmental reasons (CaF_2, Na_2O).
- The L_P equation had no temperature adjustment term.
- The L_P equation has since been reviewed and updated.

The thirty six models selected (equations 10-46 in Table 1) all used common representations of basicity and oxygen potential to predict the final L_P. The L_p equations were evaluated against dataset 3. Performance of the L_P equations was evaluated by comparing the coefficient of determination (R^2) for the predicted against measured L_P values when the line of best fit was constrained to pass through the origin, as calculated by equation (8).

$$R^2 = \frac{\sum(y_i)^2 - \sum(\hat{y_i} - y_i)^2}{\sum(y_i)^2} \qquad (8)$$

The ten models with the highest R^2 are shown in Figure 1 and Table 2. From Figure 1 and Table 2, it was found that of the selected published models in Table 1 (equations 10-46), models (32 and 18), and were found to have the highest R^2 value when evaluated against dataset 3. These ten models use ($\%Fe_t$), (%FeO), [%C] or combination of to represent oxygen potential. None of the models utilising the EMF [%O] (23, 24, 27, 29, 34, 36, 38) were ranked in the top 10.

3.2 Development and Testing of a New Phosphorus Partition Model

Numerous methods of representing the oxygen potential ([O], [C], total slag Fe or a combination) and basicity (optical basicity, basicity ratios or various lime equivalents) exist as shown by the published L_P equations in Table 1. In order to test the best representation for each of the key variables, a series of new L_P models were developed, as shown in Table 3 and Figure 2. The first set of models was used to find the best representation of oxygen potential (equations 47-49 in Table 3). This was followed by a series of equations (50-55) used to examine the different representations of basicity. Each equation in Table 3 was of the general form:

$$\log L_p = \sum A_i(basicity\ term\ i) + \frac{B}{T} + \sum C_i(oxygen\ potential\ term\ i) + D \qquad (9)$$

where the coefficients A_i, B, C_i and D used in each model were determined using a root mean square minimisation approach on dataset 2. The new models were tested on dataset 3 and the R^2 values (Table 3) were calculated and compared to the published models.

All of the L_P models were developed assuming the measured L_P had an inverse relationship with temperature as shown by the majority of models in Table 1. In order to examine the best representation of oxygen potential (slag Fe_t, log[O] and [C]), the basicity was assumed to be defined by the V-ratio aim (equation (4)) in models (47-49). Model (49), which used a combination of log(Slag %Fe_t) and the final [%C] was found to have the highest R^2 value for dataset 3. Thus, the oxygen potential representation from model (49) was used in subsequent models.

Various basicity representations (V-ratio aim, V-ratio measured, (%CaO), log(%CaO), $(\%CaO)_{equivalent}$, and Λ) were tested used in the L_P models given by equations (50-55, Table 3). A comparison of these different L_P models (50-55) found model (53) had the highest R^2 for dataset 3 using log(V ratio – 0.165(%MgO)) to represent slag basicity.

3.3 Assessing the Effect of Minor Slag Constituents on the Measured L_P

To help assess the effects of minor slag constituents, dataset 1 was split into narrow ranges of temperature, basicity and oxygen potential, producing 27 small datasets. The basicity and oxygen potential terms from L_P model (53) were used due to the model's degree of fit to the industrial data. The three largest datasets (292, 1774 and 3253 heats respectively) were selected for further testing, where these datasets are defined in Table 4. Constraining the data to these narrow ranges of temperature, basicity and oxygen potential allowed evaluation of correlations between the measured L_P and minor slag constituents (TiO_2, Al_2O_3 and V_2O_5). The effects of (TiO_2), (Al_2O_3) and (V_2O_5) on the measured L_P were plotted in Figure 3.

The slag Al_2O_3 content was found to have a negative effect on the measured L_P at higher oxygen potentials in the range 0.81-0.93 (datasets 5 and 6, Table 4). At the lower oxygen potential range of 0.75-0.81 (dataset 4, Table 4) Al_2O_3 was found to correlate with increasing L_P (Figure 3b). The TiO_2 and V_2O_5 content were both found to have negative effects on the L_P (see Figure 3 a) and c)).

4. Discussion

4.1 Evaluation of Published Phosphorus Partition Relations

The published models all gave a low R^2 value when compared against dataset 3 (Figure 1 and Table 2). This may be expected for a variety of reasons, including:

- Laboratory equilibrium L_P models often have poor performance when applied to industrial datasets due to the non-equilibrium nature found in many studies, including a recent work by Assis and Fruehan[24]. This is unsurprising and is due to varying kinetic conditions (e.g. changing slag mass due to hot metal [Si], differences in blowing practice between plant operators, changing stirring conditions with lining and lance wear). As industrial phosphorus removal is often kinetically limited, laboratory models developed using equilibrium data (models 11, 22 and 31), may over-predict the actual L_P achieved.
- L_P models developed using kinetically limited, non-equilibrium industrial data will likely be plant specific due to the significant variation in the effective equilibria achieved under different kinetic conditions and operating practices. Thus, industrial L_P models are likely to have a limited fit to other industrial datasets.

- Limitations of empirical models constraining their applicability to the slag and metal composition range from which they were developed. Many heats in dataset 3 may fall outside the suitable composition ranges for some of the published models.
- Different sampling methods may have increased variation in industrially measured L_P. Slag and metal sampling can either be done simultaneously via a sub-lance, or a chill/dip sample of slag may be taken up to 10 minutes later during tapping. Irregular sampling patterns will introduce more variability into the measured L_P as the dephosphorisation reaction can continue to occur during the interval between sampling of the metal and slag. The other issue is how representative slag sampling via the sub-lance is vs. chill/ dip sampling.

Dephosphorisation is a heterogeneous reaction and it is generally considered that it is the oxygen potential at the metal-slag interface that is important for the reaction. For the current study, this can be considered to be a function of the ($\%Fe_t$), [%C] or a combination of both. The interfacial oxygen potential has been extensively studied[4, 5, 10-13, 97-100]. It is generally accepted it is controlled by a combination of both the metal and slag phases in highly stirred conditions. This oxygen potential can be represented as a balance between reactions (or equivalent slag metal reactions with oxygen in the gas phase) in equations (56) and (57).

$$(Fe_xO_y) = xFe_{(l)} + y[O] \quad (56)$$
$$[C] + [O] = CO_{(g)} \quad (57)$$

Recent work by Gu et. al.[98] focussed on iron droplet reactivity in a steel-slag-gas emulsion found dephosphorisation of the droplets was limited by mass transport in the metal phase. This is a relatively new and interesting finding and is the subject of much ongoing research.

Given the current understanding of dephosphorisation and the weight of literature suggesting the optimum representation of oxygen potential in the L_P models would be a combination of [C] and ($\%Fe_t$), this approach was utilised for developing the new L_P models in Table 3. Further, on review of the published models (10-46), models (32) and (18), utilising this approach, were found to have the highest R^2 for dataset 3.

In the future inclusion of kinetic terms that represent the degree of mixing or droplet generation in response to blowing regimes or other may improve the fit (R^2) of the L_P models, however this is beyond the scope this study.

The majority of the 10 models with the highest R^2 values only considered the slag compositional effects of CaO, MgO, Fe_tO and P_2O_5 on L_P. However, the high R^2 values of models (22, 11 and 31) also incorporated MnO, Al_2O_3, TiO_2, V_2O_5 and SiO_2, suggesting these oxides may also have a significant effect on the L_P. Hence, further investigation into the effect of these oxides and minor slag constituents on the L_P may be required.

4.2 Evaluation of New Phosphorus Partition Relations

A series of new models (47-55) were developed and fitted to dataset 2 to test the effect of different representations of oxygen potential and basicity on the comparison between calculated and measured phosphorus removal. The performance of the models was assessed using the R^2 value when tested on dataset 3. The highest R^2 value achieved by both the published and new models was 0.975, using models (32) and (53). Unsurprisingly both of these models have very similar representations for basicity and oxygen potential. Model (53) has the advantage of incorporating the effect of MgO. Steelmakers routinely add MgO as dolomite to protect the BOS refractories. Incorporating MgO in the model allows for any effect of this addition on phosphorus removal to be determined.

The effects of MnO, P_2O_5, Al_2O_3, V_2O_5 and TiO_2 were not included in any of the new L_P models developed, with the exception of the models using an optical basicity term. However, the high R^2 values of the published models incorporating these oxides, models (22, 11 and 31), suggest further investigation may allow the new L_P model (53) to be improved.

4.3 Assessing the Effect of Minor Slag Constituents on the Measured L_P

As previously discussed, industrial phosphorus partitioning does not reach equilibrium due to kinetic limitations[26]. Consequently, there was significant scatter present in the data

shown in Figure 3. However, the weak correlations with slag composition (TiO_2, Al_2O_3, V_2O_5) may warrant further investigation under controlled laboratory conditions.

At higher oxygen potentials, the slag Al_2O_3 content was found to have a negative effect on the measured L_P. In contrast, at low oxygen potentials, Al_2O_3 was found to correlate with increasing L_P (Figure 3b). Al_2O_3 has little effect on the oxygen potential for dephosphorisation as it typically enters the BOS as carryover slag from the blast furnace or desulphurisation pre-treatment. Al_2O_3 is amphoteric, thus adding Al_2O_3 to a basic slag will result in it forming a complex anion therefore it will have an acid oxide character[101, 102]. Therefore Al_2O_3 has a negative effect on the slag basicity and subsequently is expected to decrease the measured L_P. CaO dissolution in basic slags increases with Fe^{2+}, Mn^{2+} and Mg^{2+} content[103]. At low oxygen potentials there is less Fe_tO and MnO available to aid in CaO dissolution. Al_2O_3 also increases CaO dissolution, thus it is speculated that the correlation between Al_2O_3 and L_P at low oxygen potentials is due to increased CaO dissolution and subsequently higher basicity.

The TiO_2 and V_2O_5 content of slag are highly correlated, thus it was expected that both oxides would display similar correlations with the measured L_P, as shown in Figure 3 a) and c). These oxides were found to decrease the measured L_P with the correlation becoming more pronounced at lower oxygen potentials. This negative correlation is in good agreement with some literature as both [V] and [Ti] reduce the oxygen potential and [P] activity[104], thereby potentially inhibiting the dephosphorisation reaction, given in equation (1).

Selin[41, 42, 48] investigated the effect of Al_2O_3, TiO_2 and V_2O_5 additions on dephosphorisation in EAF steelmaking slags. Although EAF slags generally have a lower basicity, these slags overlap with the lower basicity ranges of industrial BOS slags. Selin[43,44,49] found Al_2O_3, TiO_2 and V_2O_5 all increased the slag phosphate capacity. However, their effects were at least partly counteracted by a significant decrease in the oxygen potential. This resulted in a moderate increase in L_P when SiO_2 was replaced with TiO_2 and V_2O_5. The results with Al_2O_3 varied. This increase in phosphate capacity may help offset the effect of vanadium and

titanium on oxygen potential and may explain the smaller negative correlation of TiO_2 and V_2O_5 on L_P at higher oxygen potentials seen in Figure 3a) and c).

While the thermodynamic effects of TiO_2, V_2O_5 and Al_2O_3 on L_P may be explained by the results of Selin[41, 42, 48], the effect of TiO_2 on the kinetics of dephosphorisation remains unclear. Assuming the reaction is under a mass transfer control regime, the effect of these oxides on the slag viscosity should be considered. The effect of TiO_2 on slag viscosity has been studied primarily in blast furnace slags with the data showing a decrease in viscosity of $CaO\text{-}SiO_2\text{-}TiO_2$ slags under argon atmospheres[105-115]. However, many of these studies also observed the effect of TiO_2 on the viscosity to become less pronounced with increasing temperature, basicity (i.e. becoming more like BOS process conditions) and TiO_2 content[114].

Conversely, TiO_2 additions may increase the apparent viscosity in high basicity steelmaking slags close to CaO and/or MgO saturation due to the formation of solid calcium and/or magnesium titanates in the liquid slag. Other authors have speculated this is the reason for increased slag foaming with TiO_2 content[116]. Ohno and Ross[117] also found TiO_2 additions increased the slag viscosity in $CaO\text{-}SiO_2\text{-}Al_2O_3\text{-}TiO_2$ slags under reducing atmospheres and in the presence of solid carbon due to either the reduction of (TiO_2) to [Ti] or Ti(C, N) formation. These conditions may exist in the BOS process early in the heat, before significant decarburisation of the metal has occurred, or close to the MgO-C refractory walls[118-121].

Ilmenite ($FeTiO_3$) additions to BOS slags have been found to increase slag fluidity and dephosphorisation in industrial trials. However, the exception was high carbon heats (0.4wt% C aim) which were found to have low fluidity slags and higher final [P][122]. Hence, TiO_2 is expected to increase the rate of dephosphorisation in high oxygen potential slags below CaO and MgO saturation. TiO_2 is expected to have a negative effect on the rate of dephosphorisation at low oxygen potentials and with high basicity slags due to an increase in apparent slag viscosity. This effect of TiO_2 on mass transfer may also partly explain the weaker negative correlation with L_P at higher oxygen potentials, shown in Figure 3a).

4.4 Industrial Significance

Whilst significant scatter is observed in the industrial dataset, laboratory studies[30, 37, 63, 75, 76, 82] have shown that empirical L_P models of this structure (i.e. $LogL_P$, 1/T, basicity as a V ratio or CaO equivalence, oxygen potential using slag Fe_t and/or [C]) can accurately predict the L_P under equilibrium conditions. The scatter in the industrial data is at least in part a result of kinetic effects that are not readily accounted for in the model.

While many of the process conditions in the BOS are optimised for factors other than phosphorus removal, L_P models can be used to predict slag composition effects on the L_P. Thus the L_p model can be used to help determine the required flux additions and aid development of new fluxing/blowing practices.

In practice, steelmakers start each BOF heat with aims for L_P, end point temperature, steel and slag compositions. These aims are determined by a heat and mass balance of the BOF using the mass and compositions of all charged materials (hot metal, scrap, fluxes, iron ore etc.) and the required tap specifications for the grade. Thus, steelmakers can use L_P models and the predicted end point temperature, steel and slag compositions to determine if further flux additions are required achieve the aim L_P. This would be an iterative process, as any flux additions effect the heat and mass balance, repeated until the aim L_P was achieved.

The L_P model developed in this study is fitted to the Port Kembla steelworks dataset. Thus, this model may or may not work well for other plants due to variations in the effective equilibria achieved, as discussed previously. However, the approach used and the structure of the different representations of basicity, oxygen potential and temperature would be equally applicable. Hence, this study may inform industry on the development of an empirical L_P model fitted their own plant data.

5. Conclusions

Published phosphorus partition equations were compared against a large industrial dataset. A new phosphorus partition model (Model (53)) has been developed for use with industrial data. Terms correlating with the key factors controlling dephosphorisation (temperature, basicity and oxygen potential) were evaluated by regression against the large industrial

dataset. These were found to be 1/T for temperature, log(V-ratio -0.165(%MgO)) for basicity, and slag Fe_t and metal [C] for oxygen potential.

The key factors controlling dephosphorisation (temperature, basicity and oxygen potential) were isolated using the new L_P model in order to review the effect of minor slag constituents on the measured L_P. The Al_2O_3 content was found to have a negative effect on the measured L_P, except at the low oxygen potential condition tested (dataset 4). It was speculated this is due to the effect of Al_2O_3 on CaO dissolution at low Fe_tO content.

Increasing TiO_2 and V_2O_5 content were found to decrease the measured L_P, however these correlations became less prevalent at the higher oxygen potentials tested. This may be due to the increase in the slag phosphate capacity partly offsetting the reduction in oxygen potential[41, 42, 48]. This observation may also be partly explained by lower slag viscosity increasing the rate of mass transfer. TiO_2 is known to decrease slag viscosity when the slag is not saturated in CaO or MgO.

Acknowledgements

The authors would like to acknowledge the support of the ARC Research Hub for Australian Steel Manufacturing. This work is being carried out as part of a project on “The Effect of Titanium on the Kinetics of Phosphorus Removal during BOS Steelmaking”.

This research has been conducted with the support of the Australian Government Research Training Program Scholarship.

References

1. Y. Ghobara and I. Cameron, *Iron & Steel Technology*, 2017, **14**(4), 80-89.
2. W. Urban, M. Weinberg, and J. Cappel, *Stahl Eisen*, 2014, **134**(8), 27-39.
3. E. T. Turkdogan, *ISIJ Int.*, 2000, **40**(10), 964-970.
4. B. J. Monaghan, R. J. Pomfret, and K. S. Coley, *Metall. Mater. Trans. B*, 1998, **29B**(1), 111-118.
5. B. Monaghan: 'Kinetics of hot metal dephosphorization using lime based slags', PhD thesis, University of Strathclyde, Glasgow, 1996.
6. E. T. Turkdogan: 'Pretreatment of Blast Furnace Iron', in 'Fundamentals of steelmaking', 200-208; 1996, London, Institute of Materials.
7. E. T. Turkdogan: 'Oxygen Steelmaking', in 'Fundamentals of steelmaking', 209-244; 1996, London, Institute of Materials.
8. T. Tamura and M. Hino: 'Development of New Dephosphorus Flux Using Two Liquid Slag Phases in the secondary refining Process', ICS, 2005, AIST.
9. A. Ghosh: 'Secondary Steelmaking: Principles and Applications'; 2000, Taylor & Francis.
10. P. Wei, M. Sano, M. Hirasawa, and K. Mori, *ISIJ Int.*, 1993, **33**(4), 479-487.
11. P. Wei, M. Ohya, M. Hirasawa, M. Sano, and K. Mori, *ISIJ Int.*, 1993, **33**(8), 847-854.
12. K. Gu, N. Dogan, and K. Coley: 'Kinetics Of Phosphorus Mass Transfer And The Interfacial Oxygen Potential For Bloated Metal Droplets During Oxygen Steelmaking', Molten 2016: X International Conference on Molten Slags, Fluxes and Salts, Seattle, Washington, USA, 2016, John Wiley & Sons, Inc., Hoboken, New Jersey

TMS (The Minerals, Metals & Materials Society), 989-998.

13. G. Brooks, K. Coley, N. Dogan, M. A. Rhamdhani, B. Rout, Z. Li, and J. W. K. Van Boggelen: 'Bloated droplet theory: A new approach to understanding oxygen steelmaking', AISTech 2016 Iron and Steel Technology Conference, 2016, Association for Iron and Steel Technology, AISTECH, 1047-1053.
14. K. Gu, B. Jamieson, N. Dogan, and K. Coley: 'Kinetics of Dephosphorisation and the Interfacial Oxygen Potential for Bloated Metal Droplets During Oxygen Steelmaking', AISTech 2015 Iron and Steel Technology Conference, Cleveland, Ohio, USA, May 4-7th 2015, 2015, Association for Iron and Steel Technology, AISTECH, 2148-2155.
15. E. Chen and K. S. Coley, *Ironmaking Steelmaking*, 2010, **37**(7), 541-545.
16. K. Coley, F. Ji, G. Brooks, and A. Rhamdahni: 'The Interface in Slag Reactions; A Moving Target', Molten 2009: VIII International Conference on Molten Slags, Fluxes and Salts, Santiago, Chile, 19-21 January 2009, 2009, GECAMIN, 727-735.
17. E. Chen and K. Coley: 'Kinetics Study of Droplet Swelling in BOF Steelmaking', Molten 2009: VIII International Conference on Molten Slags, Fluxes and Salts, Santiago, Chile, 19-21 January 2009, 2009, GECAMIN.
18. K. C. Mills: 'Basicity and optical basicities of slags', in 'Slag atlas (2nd Edition)', (ed. V. D. E. (VDEh)), 2nd ed edn, 9-20; 1995, Düsseldorf, Verlag Stahleisen GmbH.
19. R. Selin: 'Studies on the MgO solubility in complex steelmaking slags in equilibrium with liquid iron and distribution of phosphorus and vanadium between slag and metal at MgO saturation', 3rd International Conference on Molten Slags and Fluxes, Glasgow, 27-29 June 1988, 1988, The Institute of Metals, 317-322.
20. M. A. Tayeb, R. Fruehan, and S. Sridhar: 'De-phosphorization in the DRI-EAF steelmaking and the effect of alumina', AISTech 2014 Iron and Steel Technology Conference, Indianapolis, IN, 2014, Association for Iron and Steel Technology, AISTECH, 1073-1086.
21. M. Tayeb, S. Spooner, and S. Sridhar, *JOM*, 2014, **66**(9), 1565-1571.
22. K. Chattopadhyay, S. Kumar, and S. Mostaghel: 'Thermodynamic analysis for developing strategies for the production of low phosphorous steel grades', Materials Science and Technology Conference and Exhibition 2013, MS and T 2013, Montreal, QC, 2013, 590-601.
23. K. Chattopadhyay and S. Kumar: 'Application of thermodynamic analysis for developing strategies to improve BOF steelmaking process capability', AISTech 2013 Iron and Steel Technology Conference, Pittsburgh, PA, 2013, 809-819.
24. A. N. Assis and R. J. Fruehan: 'Phosphorus removal in oxygen steelmaking: A comparison between plant and laboratory data', AISTech 2013 Iron and Steel Technology Conference, Pittsburgh, PA, 2013, 889-895.
25. A. N. Assis, R. J. Fruehan, and S. Sridhar: 'Phosphorus equilibrium between liquid iron and $CaO-SiO_2$-MgO-FeO slags', AISTech 2012 Iron and Steel Technology Conference and Exposition, Atlanta, GA, 2012, 861-870.

26. K. Sipos and E. Alvez: 'Dephosphorization in BOF Steelmaking', Molten 2009: VIII International Conference on Molten Slags, Fluxes and Salts, Santiago, Chile, 19-21 January 2009, 2009, GECAMIN, 1023-1030.
27. S. Basu, A. K. Lahiri, and S. Seetharaman, *ISIJ Int.*, 2007, **47**(8), 1236-1238.
28. S. Basu, A. K. Lahiri, and S. Seetharaman, *Metall. Mater. Trans. B*, 2007, **38B**(4), 623-630.
29. S. Basu, A. K. Lahiri, and S. Seetharaman, *Metall. Mater. Trans. B*, 2007, **38B**(3), 357-366.
30. C. M. Lee and R. J. Fruehan, *Ironmaking Steelmaking*, 2005, **32**(6), 503-508.
31. Y. Ogawa, M. Yano, S. Y. Kitamura, and H. Hirata, *Steel Res. Int.*, 2003, **74**(2), 70-76.
32. Y. Ogawa, M. Yano, S. Kitamura, and H. Hirata, *Tetsu To Hagane*, 2001, **87**(1), 21-28.
33. E. T. Turkdogan, *ISIJ Int.*, 2000, **40**(9), 827-832.
34. I. H. Jung, J. D. Seo, and S. H. Kim, *Steel Res*, 2000, **71**(9), 333-339.
35. K. Ide and R. J. Fruehan, *Iron Steelmaker I and SM*, 2000, **27**(12), 65-70.
36. H. Ishii and R. J. Fruehan, *Iron Steelmaker I and SM*, 1997, **24**(2), 47-54.
37. H. Suito and R. Inoue, *ISIJ Int.*, 1995, **35**(3), 258-265.
38. R. W. Young, J. A. Duffy, G. J. Hassall, and Z. Xu, *Iron and Steelmaking*, 1992, **19**(3), 201-219.
39. R. W. Young: 'Use of the optical basicity concept for determining phosphorus and sulphur slag/metal partitions', 13176, European Commission, Luxemburg, 1991.
40. T. Usui, K. Yamada, Y. Kawai, S. Inoue, H. Ishikawa, and Y. Nimura, *Tetsu-to-Hagane*, 1991, **77**(10), 1641-1648.
41. R. Selin, *Scand. J. Metall.*, 1991, **20**(5), 279-299.
42. R. Selin, *Scand. J. Metall.*, 1991, **20**(6), 318-328.
43. E. Schurmann and H. Fischer, *Steel Res*, 1991, **62**(7), 303-313.
44. R. Selin, Y. Dong, and Q. A. Wu, *Scand. J. Metall.*, 1990, **19**(3), 98-109.
45. T. A. Boom, D. R. Foshnacht, and D. M. Haezebrouck, *Iron Steelmaker I and SM*, 1990, **17**(10), 59-62.
46. A. Bergman and A. Gustafsson: 'Use of optical basicity to calculate phosphorus and oxygen contents in molten iron', 3rd International Conference on Molten Slags and Fluxes, Glasgow, 27-29 June 1988, 1988, The Institute of Metals, 150-153.
47. A. Bergman, *Trans, ISIJ*, 1988, **28**(11), 945-951.
48. R. Selin: 'The role of phosphorus, vanadium and slag forming oxides in direct reduction steelmaking', PhD thesis, KTH - The Royal Institute of Technology, Stockholm, 1987.
49. K. Kunisada and H. Iwai, *Trans, ISIJ*, 1987, **27**(5), 332-339.
50. K. Kunisada and H. Iwai, *Trans, ISIJ*, 1987, **27**(4), 263-269.
51. T. Ting, H. G. Katayama, and A. Tanaka, *Tetsu-to-Hagane*, 1986, **72**(2), 225-232.
52. K. Kunisada and H. Iwai, *Trans, ISIJ*, 1986, **26**(2), 121-127.
53. K. Kunisada and H. Iwai, *Transaction of the Iron and Steel Institue of Japan*, 1986, **26**(12), B364.
54. C. Garlick, G. R. Belton, and S. Jahanshahi: 'A thermodynamic study of metal/slag phosphorus equilibria', 1986.
55. C. Bodsworth, M. Motlagh, and I. G. Nixon, *Ironmaking Steelmaking*, 1986, **13**(3), 117-125.
56. X. F. Zhang, I. D. Sommerville, and J. M. Toguri, *Trans. Iron. Steel Soc. AIME*, 1985, **6**, 29-35.
57. Y. Shirota, K. Katohgi, K. Klein, H. J. Engell, and D. Janke, *Trans, ISIJ*, 1985, **25**(11), 1132-1140.
58. K. Kunisada and H. Iwai, *Tetsu To Hagane*, 1985, **71**(1), 63-69.
59. K. Kunisada and H. Iwai, *Trans, ISIJ*, 1985, **25**, B349.
60. K. Kunisada and H. Iwai, *Trans, ISIJ*, 1985, **25**, B174.
61. H. Suito and R. Inoue, *Trans, ISIJ*, 1984, **24**(4), 257-265.
62. H. Suito and R. Inoue, *Trans, ISIJ*, 1984, **24**(1), 47-53.
63. H. Suito and R. Inoue, *Trans, ISIJ*, 1984, **24**(1), 40-46.
64. T. Mori, *Trans Jpn Inst Met*, 1984, **25**(11), 761-771.
65. K. Kunisada and H. Iwai, *Tetsu To Hagane*, 1984, **70**(14), 1681-1688.
66. Y. Kawai, R. Nakao, and K. Mori, *Trans, ISIJ*, 1984, **24**(7), 509-514.
67. K. Yamada, T. Usui, K. Iwasaki, E. Ogura, S. Kuriyama, and O. Yamase, *Tetsu-to-Hagane*, 1983, **69**(15), 1841-1848.
68. K. Yamada, K. Iwasaki, T. Usui, E. Ogura, S. Kuriyama, and O. Yamase: 'Hot metal dephosphorization by use of soda ash', 11 Developments in Hot Metal Preparation for Oxygen Steelmaking., Hamilton, Ont, Canada, 1983, McMaster Univ, Dep of Metallurgy & Materials Science, 245-267.

69. K. Kunisada and H. Iwai, *Tetsu To Hagane*, 1983, **69**(14), 1591-1598.
70. Y. Kikuchi, K. Takahashi, Y. Kawai, K. Kawakami, H. Tenma, and K. Taguchi: 'Development of ladle dephosphorization process in N.K.K*',* Scaninject III : 3rd International Conference on Refining of Iron and Steel by Powder Injection, Luleêa, Sweden, June 15-17, 1983, 1983, MEFOS, 13:11-13:21.
71. H. Suito and R. Inoue, *Trans, ISIJ*, 1982, **22**(11), 869-877.
72. T. Ikeda and T. Matsuo, *Trans, ISIJ*, 1982, **22**(7), 495-503.
73. D. R. Gaskell, *Trans, ISIJ*, 1982, **22**(12), 997-1000.
74. T. Usui, K. Yamada, Y. Miyashita, and K. Taguchi, *Tetsu-to-Hagane*, 1981, **67**, S943.
75. H. Suito, R. Inoue, and M. Takada, *Tetsu-to-Hagane*, 1981, **67**(16), 75-84.
76. H. Suito, R. Inoue, and M. Takada, *Trans, ISIJ*, 1981, **21**(4), 250-259.
77. Y. Ito, S. Sato, Y. Kawachi, and H. Tezuka, *Tetsu-to-Hagane*, 1979, **65**, S737.
78. G. J. W. Kor, *Metall. Trans. B*, 1977, **8B**(1), 107-113.
79. Y. Kawai, I. Takahashi, Y. Miyashita, and K. Tachibana, *Tetsu-to-Hagane*, 1977, **63**, S156.
80. J. F. Elliott, D. C. Lynch, and T. B. Braun, *Metall. Trans. B*, 1975, **6**(4), 495-501.
81. Y. Kawai, H. Nakajima, and K. Mori, *Transaction of the Iron and Steel Institue of Japan*, 1971, **11**, 520-523.
82. G. W. Healy, *JISI*, 1970, **208**(7), 664-668.
83. R. G. Ward: 'The Phosphorus Problem', in 'The Physical Chemistry of Iron and Steel Making', 121-135; 1962, London, Edward Arnold.
84. E. T. Turkdogan and J. Pearson, *JISI*, 1954, **176**, 59-63.
85. E. T. Turkdogan and J. Pearson, *JISI*, 1953, **175**, 393-401.
86. E. T. Turkdogan and J. Pearson, *JISI*, 1953, **173**, 217-223.
87. H. Flood and K. Grojotheim, *JISI*, 1952, **171**, 64-70.
88. P. Herasymenko and G. E. Speight, *JISI*, 1950, **166**, 169-183.
89. P. Herasymenko and G. E. Speight, *JISI*, 1950, **166**, 289-303.
90. P. Vajragupta, *JISI*, 1948, **158**, 494-496.
91. K. Balajiva and P. Vajragupta, *JISI*, 1947, **155**(4), 563-567.
92. T. B. Winkler and J. Chipman, *Transactions of AIME*, 1946, **167**, 111-133.
93. K. Balajiva, A. G. Quarrell, and P. Vajragupta, *JISI*, 1946, **153**, 115-145.
94. C. H. Herty, *Transactions of AIME*, 1926, **73**, 1107-1134.
95. H. Gaye, J. Lehmann, D. Kirner, and D. Janke: 'Sulphide capacities, Phosphate and phosphide capacities in metallurgical slags', in 'Slag atlas (2nd Edition)', (ed. V. D. E. (VDEh)), 2nd ed edn, 257-281; 1995, Düsseldorf, Verlag Stahleisen GmbH.
96. E. T. Turkdogan: 'Fundamentals of steelmaking'; 1996, London, Institute of Materials.
97. K. Gu, N. Dogan, and K. S. Coley, *Metall. Mater. Trans. B*, 2017.
98. K. Gu, N. Dogan, and K. S. Coley, *Metall. Mater. Trans. B*, 2017, 1-12.
99. K. Gu, N. Dogan, and K. S. Coley, *Metall. Mater. Trans. B*, 2017.
100. B. K. Rout, G. Brooks, Subagyo, M. A. Rhamdhani, and Z. Li, *Metall Mat Trans B Process Metall Mat Process Sci*, 2016, **47**(6), 3350-3361.
101. H. Abdeyazdan: 'The Wettability, Interfacial Tension and Dissolution of Alumina, Spinel and Calcium aluminate with/in Ladle and Tundish Slags', PhD thesis, University of Wollongong, Wollongong, 2016.
102. K. C. Mills: 'Structure of liquid slags', in 'Slag atlas (2nd Edition)', (ed. V. D. E. (VDEh)), 2nd ed edn, 1-8; 1995, Düsseldorf, Verlag Stahleisen GmbH.
103. Z. Li, M. Whitwood, S. Millman, and J. v. Boggelen: 'Dissolution of lime into BOS slag: from laboratory experiment to industrial converter*',* Molten 2012: IX International Conference on Molten Slags, Fluxes and Salts, Beijing, China, 2012, The Chinese Society for Metals.
104. Anon: 'Thermodynamic data for steelmaking', 264; 2010, Tohoku University Press.
105. Y. L. Zhen, G. H. Zhang, and K. C. Chou, *Metall. Mater. Trans. B*, 2015, **46**(1), 155-161.
106. Y. Sun, K. Zheng, J. Liao, X. Wang, and Z. Zhang, *ISIJ Int.*, 2014, **54**(7), 1491-1497.
107. K. Zheng, Z. Zhang, L. Liu, and X. Wang, *Metall. Mater. Trans. B*, 2014, **45**(4), 1389-1397.
108. Y.-L. Zhen, G.-H. Zhang, and K.-C. Chou, *ISIJ Int.*, 2014, **54**(4), 985-989.
109. Q. Shu, Z. Wang, J. L. Klug, K. Chou, and P. R. Scheller: 'Effects of B_2O_3 and TiO_2 on crystallization behavior of some slags in Al_2O_3-CaO-MgO-Na_2O-SiO_2 system*',* Molten 2012: IX International Conference on Molten Slags, Fluxes and Salts, Beijing, China, 2012, The Chinese Society for Metals.
110. Z. Wang, Q. Shu, and K. Chou: 'Study on structure characteristics of B_2O_3 and TiO_2-bearing F-free mold flux by raman spectroscopy*',* Molten 2012: IX International Conference on Molten Slags, Fluxes and Salts, Beijing, China, 2012, The Chinese Society for Metals.

111. H. Park, J. Y. Park, G. H. Kim, and I. Sohn, *Steel Res. Int.*, 2012, **83**(2), 150-156.
112. I. Sohn, W. Wang, H. Matsuura, F. Tsukihashi, and D. J. Min, *ISIJ Int.*, 2012, **52**(1), 158-160.
113. J. Li, Z. Zhang, L. Liu, W. Wang, and X. Wang, *ISIJ Int.*, 2013, **53**(10), 1696-1703.
114. J. L. Liao, J. Li, X. D. Wang, and Z. T. Zhang, *Ironmaking & Steelmaking*, 2012, **39**(2), 133-139.
115. R. Wang, M. Guo, M. Zhang, and X. Wang: 'Viscosity measurements and estimation of high TiO_2 containing blast furnace slags*',* Molten 2009: VIII International Conference on Molten Slags, Fluxes and Salts, Santiago, Chile, 19-21 January 2009, 2009, GECAMIN.
116. S.-M. Jung and R. J. Fruehan, *ISIJ Int.*, 2000, **40**(4), 348-355.
117. A. Ohno and H. Ross, *Can. Metall. Q.*, 1963, **2**(3), 259-279.
118. W. E. Lee and S. Zhang: 'Direct and indirect slag corrosion of oxide and oxide-c refractories*',* VII International Conference on Molten Slags Fluxes and Salts, Cape Town, South Africa, 2004, The South African Institute of Mining and Metallurgy, 309-319.
119. W. E. Lee and S. Zhang, *Int. Mater. Rev.*, 1999, **44**(3), 77-104.
120. Z. Yuan, Y. Wu, H. Zhao, H. Matsuura, and F. Tsukihashi, *ISIJ Int.*, 2013, **53**(4), 598-602.
121. A. Yamaguchi, *Taikabutsu Overseas*, 1984, **4**(1), 32-37.
122. S. K. Sharma and T. W. Miller: 'Evaluation of fluorspar substitutes*',* 57th National Open Hearth and Basic Oxygen Steel Conference, Atlantic City, April 28 - May 1, 1974, Metallurgical society of the american institute of mining, metallurgical, and petroleum engineers, 178-198.

Figures & Captions

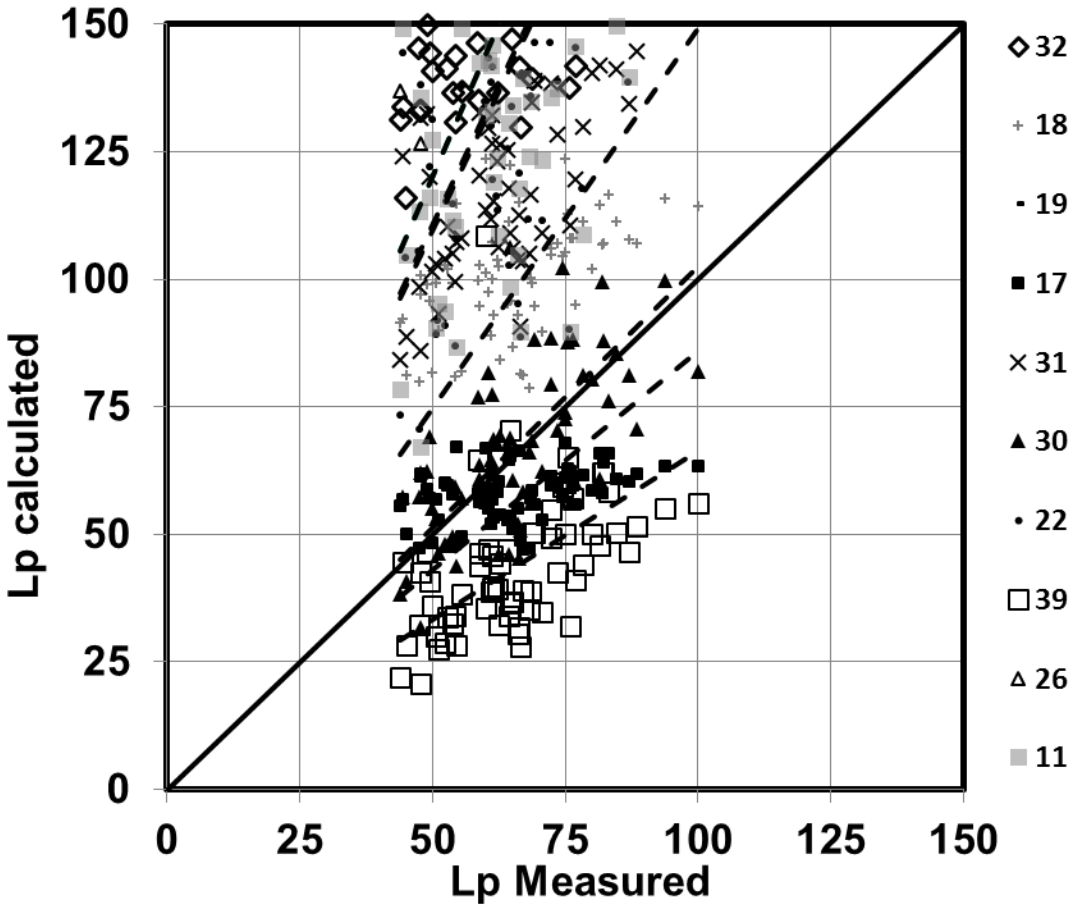

Figure 1: L_P calculated vs. L_P measured for top 10 models by R^2 over dataset 3.

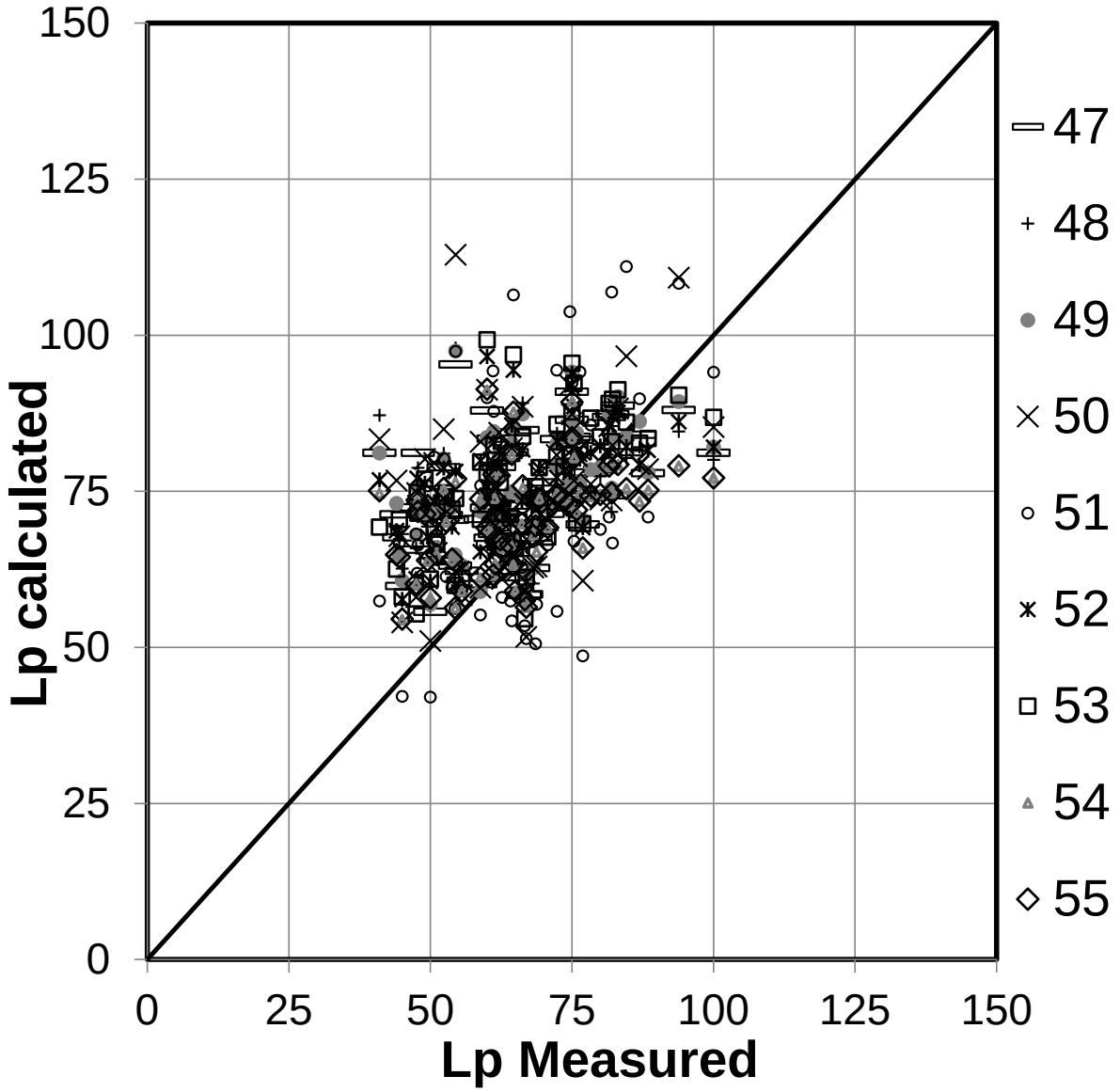

Figure 2: L_P calculated vs. L_P measured for new L_P models developed

a)

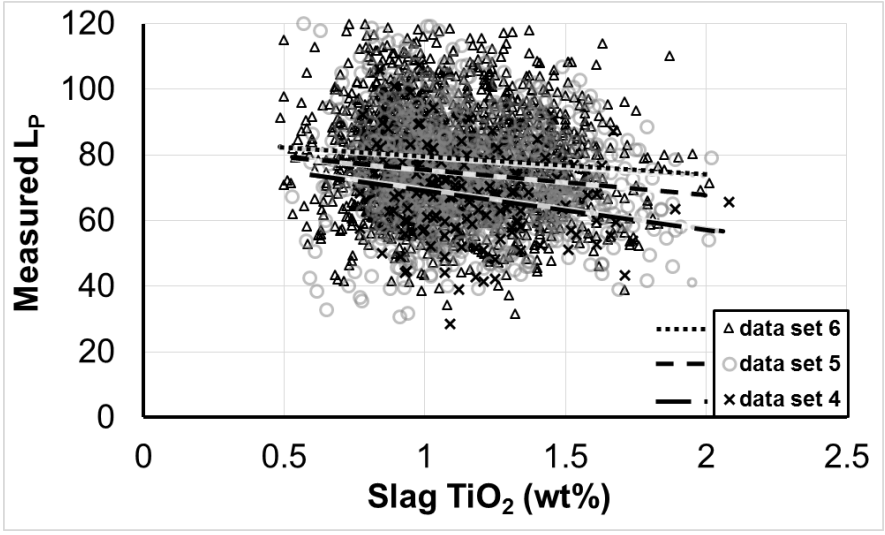

b)

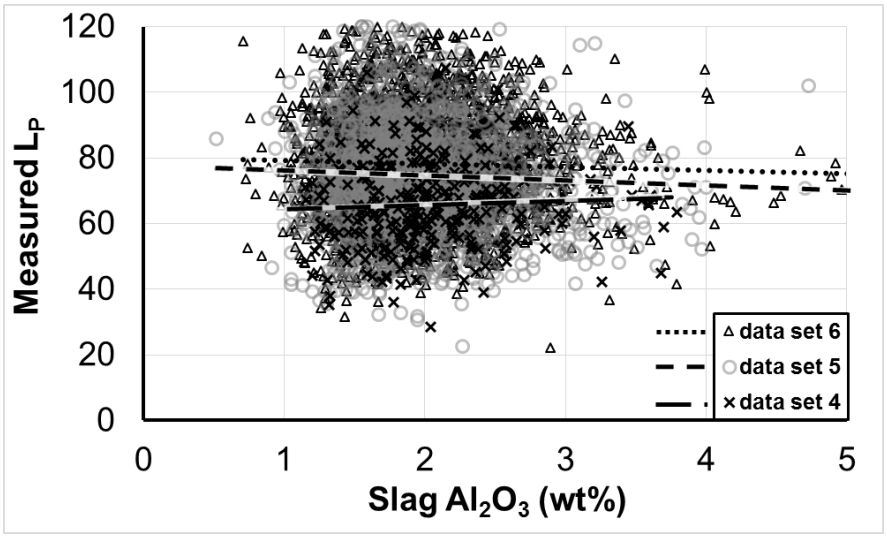

c)

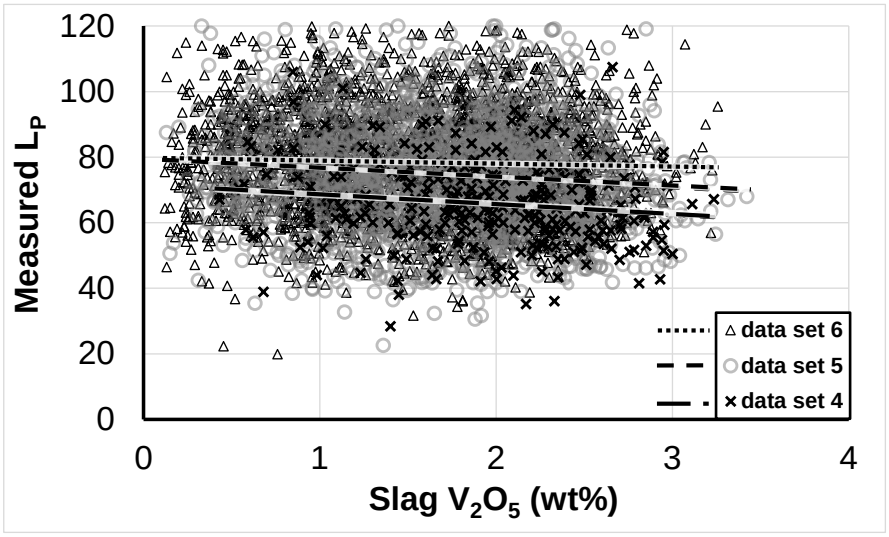

Figure 3: L_P measured vs. **a)** slag (TiO_x) mass% **b)** (Al_2O_3) mass% **c)** (V_2O_5) mass% for datasets 4-6

Tables & Captions

Table 1: A selection of L_P equations developed for slags in CaO-SiO_2-Fe_tO-P_2O_5-(MgO, MnO, Al_2O_3, TiO_2, and VO_2) systems.

Equation	**Conditions**	**No.**
$\log L_P = 0.06[(\%CaO) + 0.37(\%MgO) + 4.65(\%P_2O_5) - 0.05(Al_2O_3) - 0.2(\%SiO_2)] + \frac{11570}{T} - 10.52 + 2.5\log(\%Fe_t)$	MgO-Al_2O_3, 1600°C	(10)[20, 21]
$\log L_P = 0.0680[(\%CaO)+0.42(\%MgO)+1.16(\%P_2O_5)+0.2(\%MnO)] + \frac{11570}{T} -10.520 + 2.5 \log(\%Fe_t)$	MgO-MnO, 1600-1655°C	(11)[24, 25]
$\log L_P = 0.07(\%CaO)+0.031(\%MgO)+0.02(\%MnO)+0.31(\%Al_2O_3) + \frac{10911}{T} -11.4 + 2.84 \log(\%Fe_t)$	MgO-Al_2O_3–TiO_2-V_2O_5 1550-1667°C	(12)[23]
$\log L_P = 0.026(\%CaO)+0.092(\%MgO)+0.04(\%MnO)+0.08(\%Al_2O_3) + \frac{12217}{T} -6.29 + 0.35\log(\%Fe_t)$	MgO-Al_2O_3–TiO_2-V_2O_5 1650-1727°C	(13)[23]
$\log L_P = 0.075(\%CaO)+0.025(\%MgO)+0.14(\%MnO)+0.3(\%Al_2O_3) + \frac{6042}{T} -10.27 + 3.5 \log(\%Fe_t)$	MgO-Al_2O_3–TiO_2-V_2O_5 1550-1727°C	(14)[23]
$\log L_P = 0.431((\%CaO)/(\%SiO_2))-0.361\log(\%MgO)+ \frac{13590}{T} -5.71 + 0.384\log(\%Fe_t)$	MgO	(15)[2]
$\log L_P = 0.346((\%CaO)/(\%SiO_2))-0.144\log(\%MgO)+ \frac{10173}{T} -5.41 + 0.855\log(\%Fe_t)+0.0088*\log[\%C]$	MgO	(16)[2]
$\log L_P = \frac{9736}{T} + 0.0023(\%CaO) - 0.0094(\%MgO) - 0.1910[\%C]+ 0.00053(\%Fe_tO) -3.297$	MgO-Al_2O_3–TiO_2-V_2O_5 ~1650°C	(17)[26]
$\log L_P = \frac{11913}{T} + 0.0066(\%CaO) - 0.0123(\%MgO) - 1.2270[\%C] + 0.00426(\%Fe_tO) -4.384$	MgO-Al_2O_3–TiO_2-V_2O_5 ~1650°C	(18)[26]
$\ln L_P = \frac{20.254}{T} +0.3638\ln(\%Fe_tO)-0.0499(\%MgO)-6.299-0.82915$	MgO	(19)[2]
$\log L_P = -12.24 + \frac{20000}{T} + 2.5\log(Fe_tO) + 6.65\log\left(\frac{(\%CaO)+0.8(\%MgO)}{(\%SiO_2)+(Al_2O_3)+0.8(\%P_2O_5)}\right) +0.13[\%C]$	MgO, 1550-1580°C	(20)[30]
$\log L_P = 2.5\log(\%Fe_t) +0.0715((\%CaO) + 0.25(\%MgO)) + \frac{7710.2}{T} - 8.55 + (\frac{105.1}{T} + 0.0723)[\%C]$	MgO-MnO, 1000-1680°C	(21)[31, 32]
$\log L_P = 0.0720[(\%CaO) + 0.15(\%MgO) + 0.6(\%P_2O_5) + 0.6(\%MnO)] +2.5 \log(\%Fe_t) + \frac{11570}{T} - 10.50$	MgO, 1600°C	(22)[35]
$\log L_P = 19.05\Lambda-0.148+ 0.5[\log\sum\left(\frac{\%i}{M_i}\right) + \log(\%P_2O_5)] + 2.5\log[\%O] -2.5\frac{(-115750-4.63T)}{RT}$	MgO-Al_2O_3, 1570-1600°C	(23)[36]
$\log L_P = \frac{21740}{T} -9.87 + 0.071[(\%CaO) + 0.3(\%MgO)] + 2.5\log[\%O]$	MgO-MnO, 1600°C	(24)[3, 33, 96]

$\log L_P = \frac{13958}{T}$ -7.9517 + 2.5log(%Fe_tO)- (%Fe_tO)(1.43x10^{-2} + 1.032x10^{-4}(%Fe_tO)) -0.36		(25)[2]
$\log L_P = 5.60 \log[(\%CaO) + 0.3(\%MgO) + 0.05(\%Fe_tO)] + \frac{14800}{T} - 18.038 + 0.5\log(\%P_2O_5) + 2.5 \log(\%Fe_t)$	MgO-Al_2O_3-TiO_2 1600-1700°C	(26)[40]
$\log L_P = 2.016B' - 0.34(B')^2 + \frac{52600}{T} - 11.993 + 2.5 \log[\%O]$	MgO, 1600°C	(27)[19]
$\log L_P = 21.55\Lambda + \frac{32912}{T}$ +2.5log(% Fe_t) – 34.678	MgO-Al_2O_3-TiO_2-VO_2 1600°C	(28)[46, 47]
$\log L_P = 21.55\Lambda + \frac{32912}{T}$ - 27.90 + 2.5 log[%O]	MgO-Al_2O_3-TiO_2-VO_2 1550-1650°C	(29)[46, 47]
$\log L_P = 3.52 \log(\%CaO) + \frac{4977}{T+17.8}$ + 2.5log(%FeO) +0.5log(%P_2O_5) -10.46	1550-1650°C	(30)[45]
$\log L_P = 1.53126\log(\%FeO)+3.23369\log(\%CaO)-5.3505+ \log\left(\frac{1.6+\sqrt{(1.28+(\%P)-1.6(0.64+(\%P))^{0.5}}}{1.820}\right)$ - $0.00129\left(\frac{(\%Al_2O_3)}{(\%Al_2O_3)+(\%SiO_2)+(\%TiO_2)+(\%VO_2)}\right)$-$0.00098\left(\frac{(\%TiO_2)}{(\%Al_2O_3)+(\%SiO_2)+(\%TiO_2)+(\%VO_2)}\right)$- $0.00026\left(\frac{(\%VO_2)}{(\%Al_2O_3)+(\%SiO_2)+(\%TiO_2)+(\%VO_2)}\right)$– 6.909 + $\frac{12940}{T}$	MgO 1600°C	(31)[41, 42, 48]
$\log L_P = 0.6639\log((\%CaO)/(\%SiO_2)) + \frac{8198.1}{T}$ -3.113 + 0.3956log(%Fe_t)-0.2075log[%C]		(32)[2]
$\log L_P = N_{Ca^{2+}}\left(\frac{144270}{T} - 36.70\right) + N_{Mg^{2+}}\left(\frac{132900}{T} - 36.25\right) + N_{Mn}\left(\frac{124040}{T} - 36.450\right) + N_{Fe^{2+}}\left(\frac{118190}{T} - 25.65\right)$-$\frac{29542}{T} - \frac{(-122173-19.25T)}{RT} - 2.5\frac{(-115750-4.63T)}{RT}$+ $0.5\log(\sum N_i M_i) + \log(\%O^{2-}) - 14.12$	MgO-MnO, 1600-1680°C	(33)[54]
$\log L_P = \frac{19872}{T}$-8.566+0.0667[(%CaO)] + 2.5log[%O]	MgO- MnO, 1520-1723°C	(34)[55]
$\log L_P = \frac{11000}{T}$ +2.5log(%FeO) + $\frac{1}{T}$ [162(%CaO) + 127.5(%MgO) + 28.5(%MnO)] - 6.28 x 10^{-4} $(\%SiO_2)^2$ - 10.76	MgO-MnO, 1550-1650°C	(35)[56]
$\log L_P = 17.55\Lambda + 5.72 - \frac{21680}{T} - 1.87 + \log[\%P] + 2.5\log[\%O]$	MgO-MnO, 1550-1650°C	(36)[64]
$\log L_P = 5.89 \log(\%CaO) + 2.5 \log(\%Fe_t) + 0.5 \log(\%P_2O_5) + \frac{15340}{T} - 18.542$	MgO-Al_2O_3-TiO_2, 1300-1400°C	(37)[72]
$\ln L_P = \Lambda\left(-558.874 + \frac{2175100}{T} - \frac{1930041500}{T^2}\right) - 24.3 + 2.5\ln[\%O] + 0.36$	MgO, 1550-1650°C	(38)[73]
$\log L_P = 0.056(\%CaO) + 2.5 \log(\%Fe_t) + 0.5 \log(\%P_2O_5) + \frac{12000}{T} - 10.42$	~1600°C	(39)[77]

$\log L_P = 5.6 \log(\%CaO) + 2.5 \log(\%Fe_t) + \frac{22350}{T} - 21.876$	~1600°C	(40)[79]
$\log L_P = \frac{22350}{T} + 0.08(\%CaO) + 2.5\log(\%Fe_tO) - 16.0$	1580-1669°C	(41)[82]
$\log L_P = \frac{22350}{T} + 7\log(\%CaO) + 2.5\log(\%Fe_tO) - 24.0$	1580-1669°C	(42)[82]
$\log L_P = \frac{2625}{T} - 7.787 + \frac{1}{2}\log(\%P_2O_5) + 2.5\log(\%Fe_t)$	MgO- MnO, 1550-1660°C	(43)[84, 86]
$\log L_P = -0.56[22N_{CaO} + 15N_{MgO} + 13N_{MnO} + 12N_{FeO} - 2N_{SiO_2}] - \frac{21000}{T} + 0.5\log N_{P_2O_5} - \log[\%P] + 0.5\log(\%P_2O_5) + 12.15$	MgO- MnO, 1550-1660°C	(44)[85, 86]
$\log L_P = 5.9\log(\%CaO) + 0.5\log(\%P_2O_5) + 2.5\log(\%Fe_t) - 0.00461T + 2.0845$	MgO-MnO-Al_2O_3, 1650-1735°C	(45)[83, 90, 91, 93]
$\log L_P = 5.39\log(\%CaO) + 0.5\log(\%P_2O_5) + 2.5\log(\%Fe_t) - 0.00447T - 3.0355$	MgO-MnO-Al_2O_3, 1650-1735°C	(46)[83, 90, 91, 93]

Table 2: R^2 values for top 10 fitting models on dataset 3

R^2	Equation
0.975	32
0.973	18
0.972	19
0.969	17
0.963	31
0.942	30
0.928	22
0.927	39
0.926	26
0.926	11

Table 3: New L_P models with R^2 values from testing on dataset 3

Equation	Testing Data set 3 R^2	No.
$\log L_p = 0.0367(V \text{ ratio aim}) + \frac{13782.4}{T} - 5.656 + 0.194\log(\%Fe_t)$	0.968	(47)
$\log L_p = 0.0380(V \text{ ratio aim}) + \frac{14304}{T} - 5.616 - 0.0594\log[O]$	0.965	(48)
$\log L_p = 0.0414(V \text{ ratio aim}) + \frac{13781.5}{T} - 5.577 + 0.147\log(\%Fe_t) - 0.816[C]$	0.970	(49)
$\log L_p = 0.0623(V \text{ ratio}) + \frac{13019.2}{T} - 5.1795 + 0.109\log(\%Fe_t) - 0.780[C]$	0.960	(50)
$\log L_p = 0.0157(\%CaO) + \frac{11572.2}{T} - 5.660 + 0.724\log(\%Fe_t) - 0.714[C]$	0.951	(51)
$\log L_p = 0.429(V \text{ ratio}) + \frac{13536.1}{T} - 5.329 + 0.0432\log(\%Fe_t) - 1.009[C]$	0.971	(52)
$\log L_p = 0.242\log(V \text{ ratio} - 0.165(MgO)) + \frac{13536.1}{T} - 5.235 - 0.009\log(\%Fe_t) - 1.010[C]$	0.975	(53)
$\log L_p = 3.306\log(\Lambda) + \frac{13535.1}{T} - 4.7717 + 0.00017\log(\%Fe_t) - 0.722[C]$	0.969	(54)
$\log L_p = 1.782(\Lambda) + \frac{13528.4}{T} - 6.521 + 0.005\log(\%Fe_t) - 0.703[C]$	0.968	(55)

Table 4: Filters applied to data set 1 to obtain datasets 4-6 for testing secondary factors

Data set	Temperature Range	Basicity Range $(10^{0.243\log((\mathrm{CaO})/(\mathrm{SiO2})\ -0.165(\mathrm{MgO}))})$	Oxygen Potential Range $(10^{-0.0092\log(\%\mathrm{Fet})\ -\ 1.0098[\mathrm{C}]})$
4	1640 – 1680°C	1.08– 1.22	0.75-0.81
5	1640 – 1680°C	1.08– 1.22	0.81-0.87
6	1640 – 1680°C	1.08– 1.22	0.87-0.93